

Hard X-ray Bursts Recorded by the IBIS Telescope of the INTEGRAL Observatory in 2003-2009

© 2011 I.V. Chelovekov*, S.A. Grebenev**

*Space Research Institute, Russian Academy of Sciences, Profsoyuznaya st. 84/32, Moscow,
117997 Russia*

Published in Astronomy Letters, Vol. 37, No. 9, pp. 597-620

Abstract - To find X-ray bursts from sources within the field of view of the IBIS/INTEGRAL telescope, we have analyzed all the archival data of the telescope available at the time of writing the paper (the observations from January 2003 to April 2009). We have detected 834 hard (15-25 keV) X-ray bursts, 239 of which were simultaneously recorded by the JEM-X/INTEGRAL telescope in the standard X-ray energy range. More than 70% of all bursts (587 events) have been recorded from the well-known X-ray burster GX 354-0. We have found upper limits on the distances to their sources by assuming that the Eddington luminosity limit was reached at the brightness maximum of the brightest bursts.

Keywords: X-ray bursts, X-ray bursters.

* E-mail: chelovekov@iki.rssi.ru

**E-mail: grebenev@iki.rssi.ru

INTRODUCTION

The X-ray bursts recorded by telescopes and detectors onboard orbital astrophysical observatories are associated mainly with thermonuclear explosions on the surfaces of weakly magnetized accreting neutron stars in low-mass X-ray binaries (type-I bursts; Lewin et al. 1993). Favorable conditions for the accumulation of a fairly thick layer of accreted matter on the stellar surface and the attainment of the pressure and temperature required for thermonuclear ignition and explosive burning at its base are created only in such objects. The luminosity of such sources (X-ray bursters) at the burst time can increase by one or two orders of magnitude relative to their quiescent state, reaching a critical Eddington level $L_c \sim 2.5 \times 10^{38} (M/M_\odot)(1 - R_g/R)^{1/2}(1 + X)^{-1}$ erg s⁻¹, where M and R are the mass and radius of the neutron star, $R_g = 2GM/c^2$ is its gravitational radius, and X is the hydrogen abundance in the accreted matter.

Solar flares and cosmic gamma-ray bursts (GRBs), events from sources of recurrent flares (magnetars), and individual events related to unsteady accretion in binary systems (type-II bursts from low-mass X-ray binaries and flares from high-mass X-ray binaries with accretion from an inhomogeneous stellar wind of the companion star) are also observed in the X-ray energy range. Compared to all these events, type-I X-ray bursts and their sources are of special, independent interest to researchers, because their observational properties are very peculiar and because they carry direct information about the processes near the surface of neutron stars under conditions of super strong gravitational field and pressure, ultrahigh temperatures, and relativistic velocities. The detection of type-I bursts, along with the detection of coherent pulsations, serves as one of the most reliable criteria for identifying the nature of the compact object (a neutron star) in X-ray binaries.

The fact that bursts are commonly observed from weak X-ray sources (or transients during their low state) opens up a possibility for using them in searching for hitherto unknown bursters with persistent X-ray fluxes below the level of reliable detection by currently available wide-field X-ray instruments. Such sources can be detected only during bursts, when their X-ray luminosities increase by tens or hundreds of times for a short time¹. The INTEGRAL orbital observatory is equipped with unique wide field telescopes that allow sky fields with an area of ~ 1000 square degrees to be simultaneously studied with a flux sensitivity higher than 1 mCrab (over several hours of observations) and an angular resolution reaching several arcminutes. In addition, it devotes up to 85% of the physical time to continuous observations of the region of the Galactic center and the Galactic plane, where the bulk of the Galactic stellar mass is concentrated. Therefore, INTEGRAL is best suited for accomplishing such a task.

In this paper, to find X-ray bursts, we analyzed the time histories of the total count rate from the ISGRI detector of the IBIS telescope onboard the INTEGRAL orbital observatory in the energy range 15–25 keV based on observations during the first seven years of its in-

¹The sources themselves can also be detected accidentally, during deep observations or surveys carried out by very sensitive mirror X-ray telescopes. However, their nature is much more difficult to identify in this case.

orbit operation (February 2003- April 2009). For all of the detected bursts, we attempted to localize (using the IBIS sky mapping capabilities) and identify them with persistent X-ray sources within the field of view. We compiled a catalog of identified bursts and constructed their time histories in a softer X-ray energy range using data from the JEM-X monitor onboard the INTEGRAL observatory if this was permitted by the observational conditions. The maximum objective of this study was the detection of hitherto unknown bursters or short lived X-ray transients.

The first part of the paper containing some results of our search for bursts in the 2003-2004 data was published previously (Chelovekov et al. 2006), as were its extensions (Chelovekov et al. 2007; Chelovekov and Grebenev 2010b). An improvement in the data processing and analysis methods revealed additional weak bursts recorded in this period. Below, we provide the full list of detected bursts that we managed to localize and, in most cases, identify with known X-ray bursters.

OBSERVATIONS AND DATA ANALYSIS

The INTEGRAL international orbital gamma-ray observatory (Winkler et al. 2003) was placed in orbit by a Russian PROTON launcher on October 17, 2002 (Eismont et al. 2003). Out of the four onboard instruments, we use data from the ISGRI detector of the IBIS gamma-ray telescope (Lebrun et al. 2003) and the JEM-X monitor (Lund et al. 2003).

The ISGRI detector is an array of 128×128 semiconductor CdTe elements with the sensitivity maximum in the energy range 15-200 keV. There is a coded mask above the detector that allows it to be used not only for spectral and timing analyses of the emission but also for reconstructing the image of the sky region in the $29^\circ \times 29^\circ$ field of view of the telescope (FWZR, the fully coded area is $9^\circ \times 9^\circ$) with an angular resolution of 12 arcmin (FWHM) and localizing X-ray and gamma-ray sources to within 1-2 arcmin. The JEM-X monitor is also a telescope with a coded aperture, but it is adapted to the standard X-ray energy range 3-35 keV. A gas chamber is used as the position-sensitive detector. The 13° field of view (FWZR, the fully coded area is $4^\circ.8$ in diameter) is limited by a collimator. Since it is appreciably narrower than the IBIS field of view, many of the bursts recorded by the ISGRI detector were not observed by the JEM-X monitor. At the same time, the angular resolution of JEM-X, 3.35 arcmin, allows bright sources to be localized more accurately than it can be done by IBIS.

The procedure of searching for bursts was developed and described in detail by Chelovekov et al. (2006). The search was conducted using the time histories of the count rate for all of the events recorded by the ISGRI detector in the energy range 15-25 keV irrespective of the photon arrival direction. The time histories of the count rate for each individual INTEGRAL observation (corresponding to an individual pointing) were reproduced with a time resolution of 5 s. For this purpose, we used data from the `isgri_events.fits` files of version 2 by selecting events in the required energy range. Subsequently, we made corrections for the detector “dead” time, took into account the possible interruptions in the telemetry flow

from one or several of its modules, and ignored the photons from its “hot” pixels.

An excess of the signal-to-noise ratio $(S - \bar{S})/N$ above a preset threshold s_0 in a given time bin served as a criterion for the presence of a burst in the derived count rate time histories. Since the number of events recorded by the detector in each time bin obeys a Poisson distribution, there is a low, but finite probability $p(s_0)$ of recording a random spike even in the absence of a real burst. To filter out such random spikes, we initially set a high threshold, $s_0 = 6.0$. It ensures that the probability of recording one random burst with $(S - \bar{S})/N \gtrsim s_0$ in the entire time series being checked (with $M \sim 3.2 \times 10^7$ time bins) does not exceed $p(s_0) \times M \simeq 20\%$. Since the total count rate of the detector depends on the emission from all sources within the IBIS field of view, its mean value \bar{S} and the noise level $N = \bar{S}^2 - \bar{S}^2$ in our formulas were initially determined independently from each individual pointing. Analysis of the detector light curves showed that the count rate variability was significant even within a single observation in some sessions. Therefore, \bar{S} and N were ultimately determined for a 500-s time interval containing the time segment being analyzed. The selection of bursts made in this way was also checked manually.

Analysis of the data showed that a number of events obviously corresponding to type-I X-ray bursts from known bursters on the light curve have a statistical significance below the adopted threshold $s_0 = 6.0$. Therefore, we also made an extended selection of candidate burst events with a reduced detection threshold, $s_1 = 3.0$. As a result of this selection, the number of burst candidates reached $\gtrsim 50\,000$ (in accordance with the predictions of Poissonian statistics); subsequently, this allowed more than 380 additional bursts to be actually detected. We emphasize that all these bursts came from known bursters, because their detection significance is too low to talk about the observation of events from hitherto unknown sources. Even at such a low threshold, one may formally expect the appearance of only $p(s_1) \times M/A \simeq 4$ false events over the entire time of observations, where $A = (29^\circ/12')^2 \simeq 2.1 \times 10^4$ is the number of statistically independent (corresponding to the angular resolution) areas in the IBIS field of view. In reality, however, after integration over the entire burst time, its significance, as a rule, turned out to be higher than that determined from an individual bin near the light curve maximum.

For all of the recorded burst candidates, we reconstructed the images of the sky area in the IBIS field of view in the energy range 15–25 keV accumulated with the same exposure during and immediately before the burst using the INTEGRAL standard data processing software. We compared the statistical significances of the detection of sources in these images to reveal and identify the burst source. As an example, Fig. 1 shows the images of the sky region in the IBIS field of view reconstructed during 5 s at the brightness maximum of the burst recorded from the X-ray burster GX 354-0 on February 28, 2003, (Fig. 1a) and based on the data of the entire observation (Fig. 1b). We see from the figure that during the burst the telescope confidently recorded only the source GX 354-0 with a signal-to-noise ratio $S/N \simeq 10.5$, while the detection significance of this source reached only $S/N \simeq 6.9$ over the entire pointing.

We analyzed a total of more than 57 000 individual observations performed by the

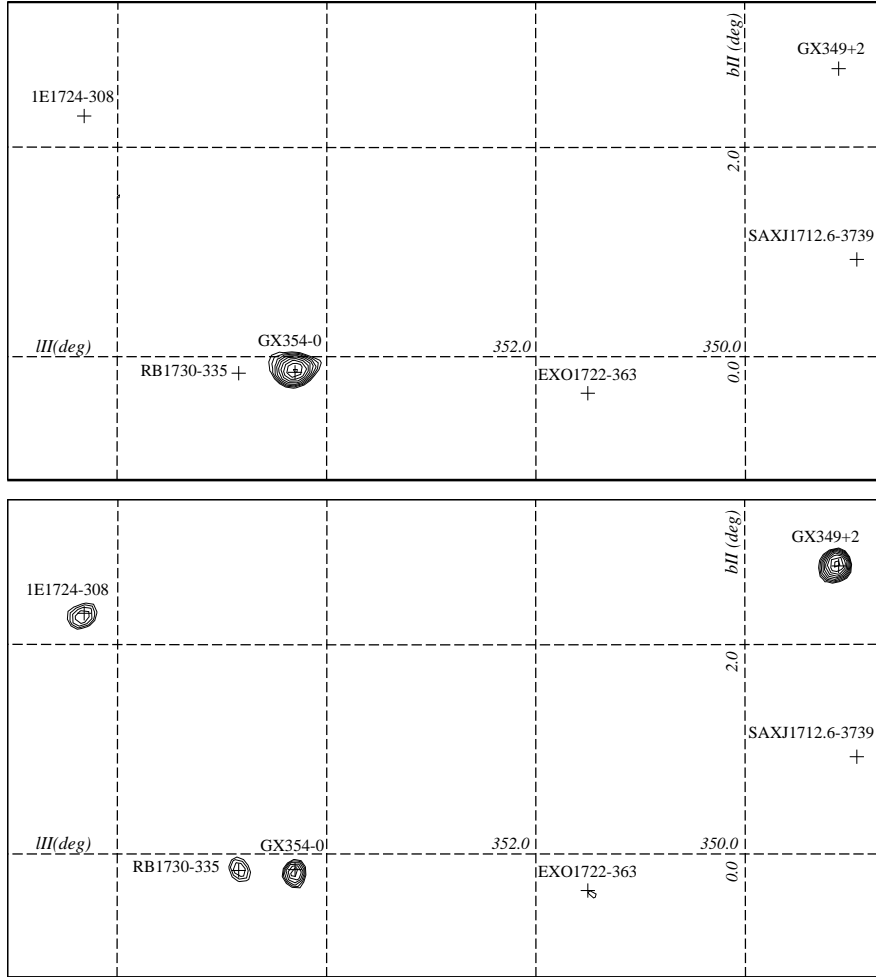


Fig. 1: IBIS/INTEGRAL source detection significance maps in the energy range 15–25 keV obtained: (a) during 5 s near the peak of the X-ray burst recorded on February 28, 2003, from the source GX 354-0 and (b) over the entire time of the corresponding INTEGRAL pointing toward this region (2185 s). Only a small $8^\circ \times 4^\circ$ part of the image in the IBIS field of view is presented. The contours indicate the signal-to-noise ratios $S/N = 3.0, 3.5, 4.1, 4.7, \dots$ (given with a logarithmic step). Except for the pulsar EXO 1733-363, all marked sources are bursters.

INTEGRAL observatory from February 10, 2003, to April 17, 2009. All these data are now in open access in the INTEGRAL archive. The duration of individual observations was typically $\sim 2.2 - 3.5$ ks; the total exposure time of all the observations used exceeded 158 Ms (~ 5 years of continuous observations).

The described set of procedures has much in common with the IBAS system of the INTEGRAL observatory: an automatic search for cosmic GRBs within the IBIS/ISGRI field of view and a wide spread of notifications of them (Mereghetti et al. 2003). The differences lie in the fact that the IBAS system (1) uses a harder and wider energy range, (2) GRB unrelated events were ignored in 2003–2004, and (3) the algorithms and programs were developed for realtime automatic work with telemetry data; therefore, they are based on very high criteria for the selection of useful events.

RESULTS

Apart from the events associated with cosmic gamma-ray bursts (recorded in the field of view or passed through the IBIS shield), solar flares, and activity of the soft gamma repeater SGR 1806-20 (more than 150 bursts), we were able to localize and, with two exceptions, to identify 834 bursts with known persistent or transient X-ray bursters. In one case, a burst was recorded from a previously unknown source in its low state that was named IGR J17380-3749 (see, e.g., Chelovekov et al. 2006, 2007; Chelovekov and Grebenev 2010a). In the second case, a burst was recorded for the first time from the known, but poorly studied source AX J1754.2-2754, which allowed the nature of this object to be recognized (Chelovekov and Grebenev 2007).

The main parameters of the localized bursts and the results of their identification are presented in the catalog of bursts (see Table 1). For each burst, the table gives: the date and time T_m of its detection (UT) - the instant at which the maximum count rate S_m is reached during this event; the burst source name; the burst duration T_{90} - the time interval during which the count rate S exceeded its mean preburst value \bar{S} by more than 10% of its peak value; the effective burst duration T_e - the ratio of the total number of counts $\Sigma(S - \bar{S})T_b$ recorded from the source over the entire burst time to the peak count rate ($S_m - \bar{S}$); and the maximum (peak) flux F_m determined for a 1 s interval. The peak fluxes F_m are given in units of the flux from the Crab Nebula². They were recalculated using the light curve (the detector count rate $S - \bar{S}$) from the absolute source flux F_5 in 5 s near the peak ($T_m - 2$ s; $T_m + 3$ s) determined from the image, i.e., applying all the required corrections (for the dead time, the observation efficiency in the incomplete coding zone, etc.). Analogous parameters are given for the bursts recorded by the JEM-X monitor simultaneously with the IBIS/ISGRI telescope: the burst duration T_{90}^j , effective duration T_e^j , and peak flux F_m^j from JEM-X data. The time of the JEM-X maximum count rate could differ from T_m . For both instruments, the time of the burst maximum, duration, effective duration, and peak flux were measured using the detector light curves with a resolution (bin length) of $T_b = 1$ s.

For each of the observed X-ray bursters, Figs. 2 and 3 present the most interesting (or characteristic) light curves measured during their bursts. The time in seconds from the beginning of the observation containing a burst is along the horizontal axis. The IBIS/ISGRI event count rate is along the vertical axis. The lower panels in Fig. 2 also show the JEM-X event count rate for the bursts recorded by the ISGRI detector. As a rule, the burst profile in the hard energy range was appreciably narrower than that in the soft one and had a more symmetric shape. We see that many bursts from the sources 4U 1724-307, Aql X- 1, 4U 1812-12, 4U 1702-429, 3A 1246-588, 4U 1608-522 and some bursts from GX 354-0 have clear signatures of photospheric expansion, including a precursor. Note, however, the unusual first precursor ~ 40 s before the main event for the burst from 4U 1608-522 recorded at 01^h36^m on February 5, 2009.

²In the energy range 15-25-keV, 1 Crab = $6.1 \times 10^{-9} \text{ ergs}^{-1} \text{ cm}^{-2}$ for a source with a power-law spectrum with a photon index $\alpha = 2.1$ or $5.8 \times 10^{-9} \text{ ergs}^{-1} \text{ cm}^{-2}$ for a source with a Wien spectrum with a temperature $kT \simeq 2.8$ keV typical of bursts with photospheric expansion.

Table 2 lists the X-ray bursters with an indication of the number of bursts recorded from each of them, the total exposure times, and the upper limits on the distances to the corresponding systems. The distances were estimated by assuming that the luminosity of the sources during the brightest bursts reached the Eddington limit and a thermonuclear flash developed in matter with a high helium abundance ($X=0$). The estimates are given only for the systems that were within the JEM-X field of view during at least one of the bursts. This allowed us to obtain the burst spectrum in a wide X-ray energy range, to fit it by a blackbody model, and to calculate the 2-100 keV flux within the framework of this model to derive a lower limit for the system's bolometric luminosity. Using such an estimate of the bolometric luminosity implies that the listed distances to the sources are only upper limits, although they were formally obtained with an accuracy better than 10%.

We see from Table 2 that more than 70% of all bursts were recorded from the same source - the well known X-ray burster GX 354-0. For a number of other bursters, the exposure time of the observations is comparable to or even larger than that of the observations for GX 354-0. Clearly, such a large number of bursts from this source is not the result of a selection effect but most likely suggests that the properties of its emission are especially "favorable" for the observation in this energy range during bursts. A detailed analysis of the bursts recorded from the source GX 354-0 in 2003-2004 by Chelovekov et al. (2006) showed that their duration in the energy range 15-25 keV was $T_{90} \sim 5 - 6$ s and the recurrence period was $\tau \sim 4$ h. We found no clear correlation between the peak flux, duration, and recurrence period of the bursts from this source.

CONCLUSIONS

We searched for "hard" X-ray bursts in the archival data of the IBIS/ISGRI detector onboard the INTEGRAL Observatory. We used the time histories of the event count rate from the entire detector in the energy range 15-25 keV. During our automated search, the criterion for detecting a positive deviation of the count rate from its mean value in one of the time bins (as a burst candidate) was an excess of the signal-to-noise ratio for this deviation above the threshold $s_0 = 3.0$. The localized bursts are listed in the catalog (Table 1); the results of their identification with one of the known (or new) bursters are also presented there. Some statistical data on the burst activity of individual bursters are given in Table 2.

It should be noted that the bursts discussed here were recorded in the hard and relatively narrow spectral range 15-25 keV and, therefore, have fairly peculiar properties. It may well be that even the most active bursters from Table 2 are also the sources of softer bursts that cannot be seen with the IBIS/ISGRI telescope. Some of the sources from the table from which we observed only single bursts are known as very active bursters in the standard X-ray energy range (Lewin et al. 1993; Grebenev et al. 2000; Emel'yanov et al. 2001; Cornelisse et al., 2003), so the content of hard bursts in them is extremely low. Therefore, the recurrence periods listed in Table 2 most likely were grossly overestimated. Note that, as follows from Table 2, the mean recurrence period of "hard" bursts from the most active burster GX 354-0,

$\tau_h \sim 1.5$ d, is much longer than the recurrence period $\tau \sim 4$ h found from the distribution of the arrival times of individual events from this burster in 2003-2004 (Chelovekov et al. 2006). Obviously, the burst activity of this burster changed greatly over seven years of its observations.

We would like to note, that the burst search algorithm we used is mainly optimized for detecting short (up to several dozens of seconds) He and H/He bursts, therefore longer events might not all be present in our catalog. For the next paper of the series we are planning to improve our algorithm and search for longer H/He and even C bursts.

As a continuation of this work, we are now searching for bursts recorded from bursters in the standard X-ray energy range by the JEM-X/INTEGRAL telescope (in the present paper, JEM-X data were used to search for and study only the counterparts of bursts recorded by IBIS). This will allow us to perform a more thorough, comprehensive, and less dependent on the selection effects (the energy range) analysis of the dependence of the burst generation rate by X-ray bursters on the accretion rate (luminosity) and to study the distribution of the number of bursts in their parameters and other correlations of parameters. The results of this study will be published in a succeeding paper.

To make our work more useful to the scientific community we are planing to open a web page with a real time access to the ISGRI/IBIS (and a bit later - the JEM-X) telescope detector lightcurves. The service will become available by the end of September 2011 at <http://hea.iki.rssi.ru/integral/>.

ACKNOWLEDGMENTS

This work is based on the INTEGRAL observational data provided via the Russian and European Science Data Centers of this observatory. The study was supported by the Program of the Russian President for support of young candidates of science (grant MK-4182.2009.2) and leading scientific schools (grant NSH-5069.2010.2), the "Origin, Structure, and Evolution of Objects in the Universe" Program of the Presidium of the Russian Academy of Sciences, and the Russian Foundation for Basic Research (grant 10-02-01466).

REFERENCES

- Altamirano et al. (D. Altamirano, N. Degenaar, J. in't Zand, et al.), ATEL #1459 (2008).
- Barret et al. (D. Barret, J. E. Grindlay, I. M. Harrus, J. F. Olive), Astron. Astrophys. 341, 789 (1999).
- Barret et al. (D. Barret, J. F. Olive, T. Oosterbroek), Astron. Astrophys. 400, 643 (2003).
- Chelovekov and Grebenev (I.V. Chelovekov and S. A. Grebenev), Pis'ma Astron. Zh. 36, 946 (2010a) [Astron. Lett. 36, 895 (2010a)]
- Chelovekov and Grebenev (I.V. Chelovekov and S. A. Grebenev), Proceedings Of Science 115, 126 (2010b).
- Chelovekov et al. (I.V. Chelovekov, S. A. Grebenev, and R. A. Sunyaev), Proceedings of the 6th Integral Workshop on The Obscured Universe, Moscow, July 2-7, 2006, Ed. by S. A. Grebenev, C.Winkler, and R. A. Sunyaev, ESA SP-622, 445 (2007).
- Chelovekov et al. (I.V. Chelovekov, S. A. Grebenev, and R. A. Sunyaev), Pis'ma Astron. Zh. 32, 508 (2006) [Astron. Lett. 32, 456 (2006)]
- Cornelisse et al. (R. Cornelisse, J. J. M. in't Zand, F. Verbunt, et al.), Astron. Astrophys. 405, 1033 (2003).
- David et al. (P. David, A. Goldwurm, T. Murakami, et al.), Astron. Astrophys. 322, 229 (1997).
- Dickey and Lockman (J.M. Dickey and F.J. Lockman), Annual Review of Astronomy and Astrophysics 28, 215 (1990).
- Di Salvo et al. (T. Di Salvo, R. Iaria, L. Burderi, N.R. Robba), The Astrophysical Journal 542, 1034 (2000).
- Eismont et al. (N. A. Eismont, A. V. Ditrikh, G. Janin et al.), Astron. Astrophys. 411, L37 (2003).
- Emel'yanov (A. N. Emel'yanov, V. A. Aref'ev, E. M. Churazov, et al.), Pis'ma Astron. Zh. 27, 908 (2001) [Astron. Lett. 27, 781 (2001)].
- Grebenev et al. (S. A. Grebenev, A. A. Lutovinov, M. N. Pavlinskii, et al.), Preprint IKI RAN, Pr-2031 (2000).
- Jonker et al. (P. G. Jonker, R. Wijnands, M. van der Klis), MNRAS 349, 94 (2004).
- Lebrun et al. (F. Lebrun, J. P. Leray, P. Lavocat, et al.), Astron. Astrophys. 411, L141 (2003).
- Lewin et al. (W. H. G. Lewin, J. van Paradijs, and R. Taam), SpaceSci. Rev. 62, 223 (1993).
- Lund et al. (N. Lund, C. Budtz-Jorgensen, N. J. Westergaard, et al.), Astron. Astrophys. 411, L231 (2003).

- Makishima et al. (K. Makishima, H. Inoue, K. Koyama, et al.), *Astron. Astrophys.* 255, 49 (1982).
- Mereghetti (S. Mereghetti, D. Gotz, J. Borkowski, et al.), *Astron. Astrophys.* 411, 291 (2003).
- Oosterbroek et al. (T. Oosterbroek, D. Barret, M. Guainazzi, E.C. Ford), *Astron Astrophys.* 366, 1380 (2001).
- Parmar et al. (A.N. Parmar, T. Oosterbroek, L. Sidoli, et al.), *Astron. Astrophys.* 380, 490 (2001).
- Sakano et al. (M. Sakano, K. Koyama, H. Murakami, et al.), *The Astrophysical Journal Supplement Series* 138, 19 (2002).
- Sidoli et al. (L. Sidoli, S. Mereghetti, G. L. Israel, et al.), *The Astrophysical Journal* 525, 215 (1999).
- Tarana et al. (A. Tarana, A. Bazzano, P. Ubertini), *The Astrophysical Journal* 688, 1295 (2008).
- Werner et al. (N. Werner, J.J.M. in't Zand, L. Natalucci, et al.), *Astron. Astrophys.* 416, 311 (2004).
- Winkler et al. (C. Winkler, T. J.-L. Courvoisier, G. Di Cocco, et al.), *Astron. Astrophys.* 411, L1 (2003).
- in't Zand et al. (J. J. M. in't Zand, F. Verbunt, E. Kuulkers, et al.), *Astron. Astrophys.* 389, 43 (2002).

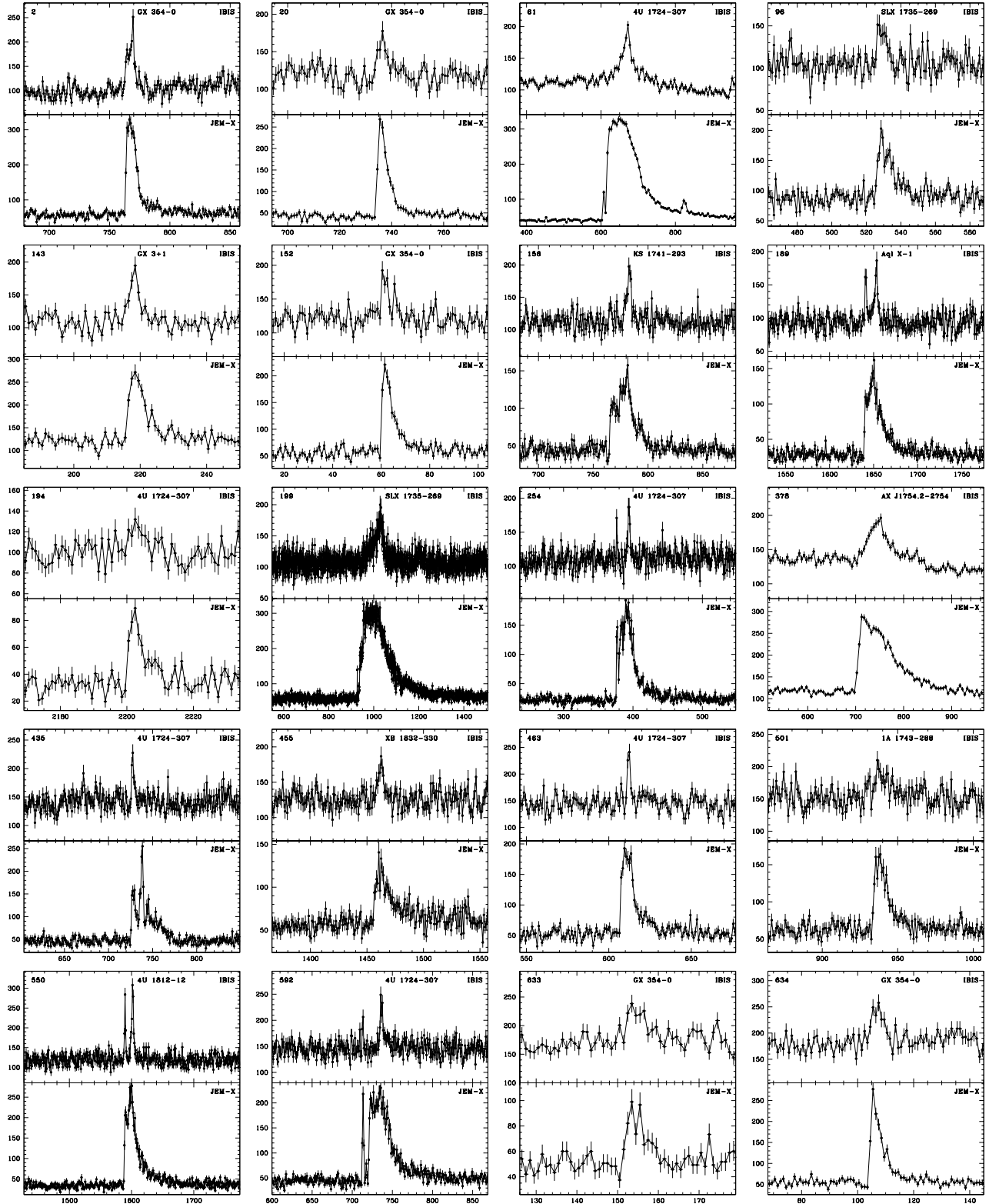


Fig. 2: Time histories of the event count rate from the ISGRI/IBIS and JEM-X telescopes aboard INTEGRAL, respectively, in the energy ranges 15-25 and 3-20 keV in the time intervals when the X-ray bursts were recorded. The time in seconds from the beginning of observation is along the horizontal axis. Each point corresponds to the count rate averaged over 1 s (5 s for bursts with a duration exceeding 30 s). The name of the X-ray burster (the burst source) is given in the upper right corner of each figure; the burst number in Table 1 is given in the upper left corner.

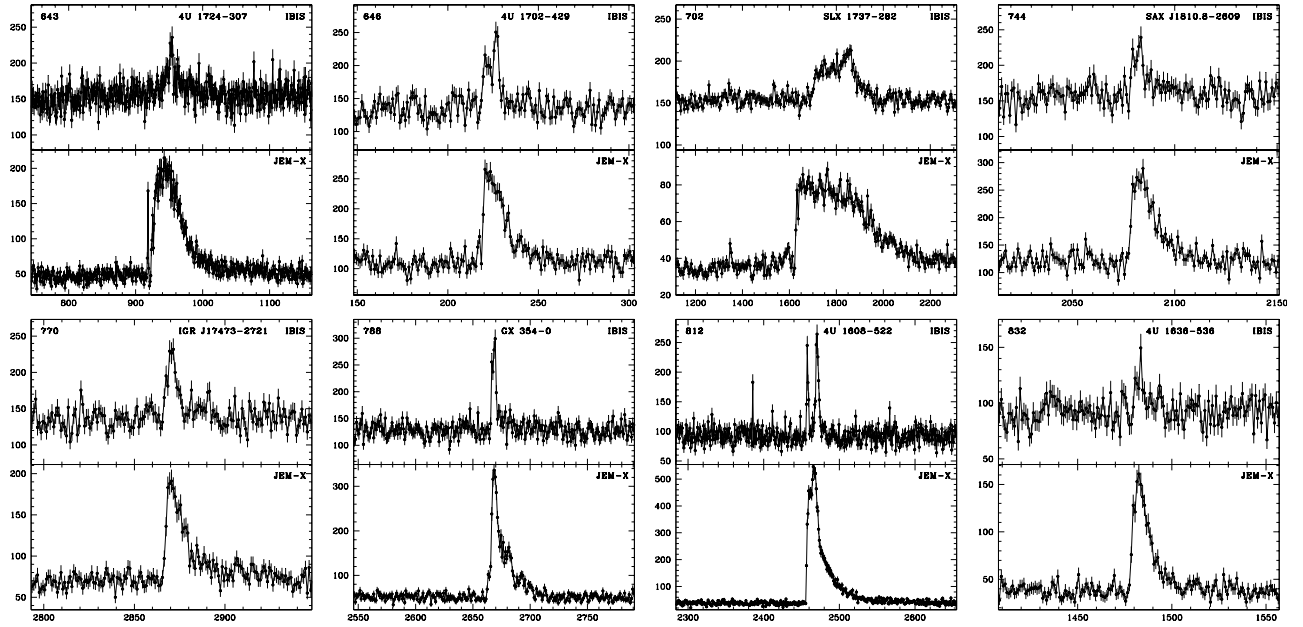


Fig. 2: Contd.

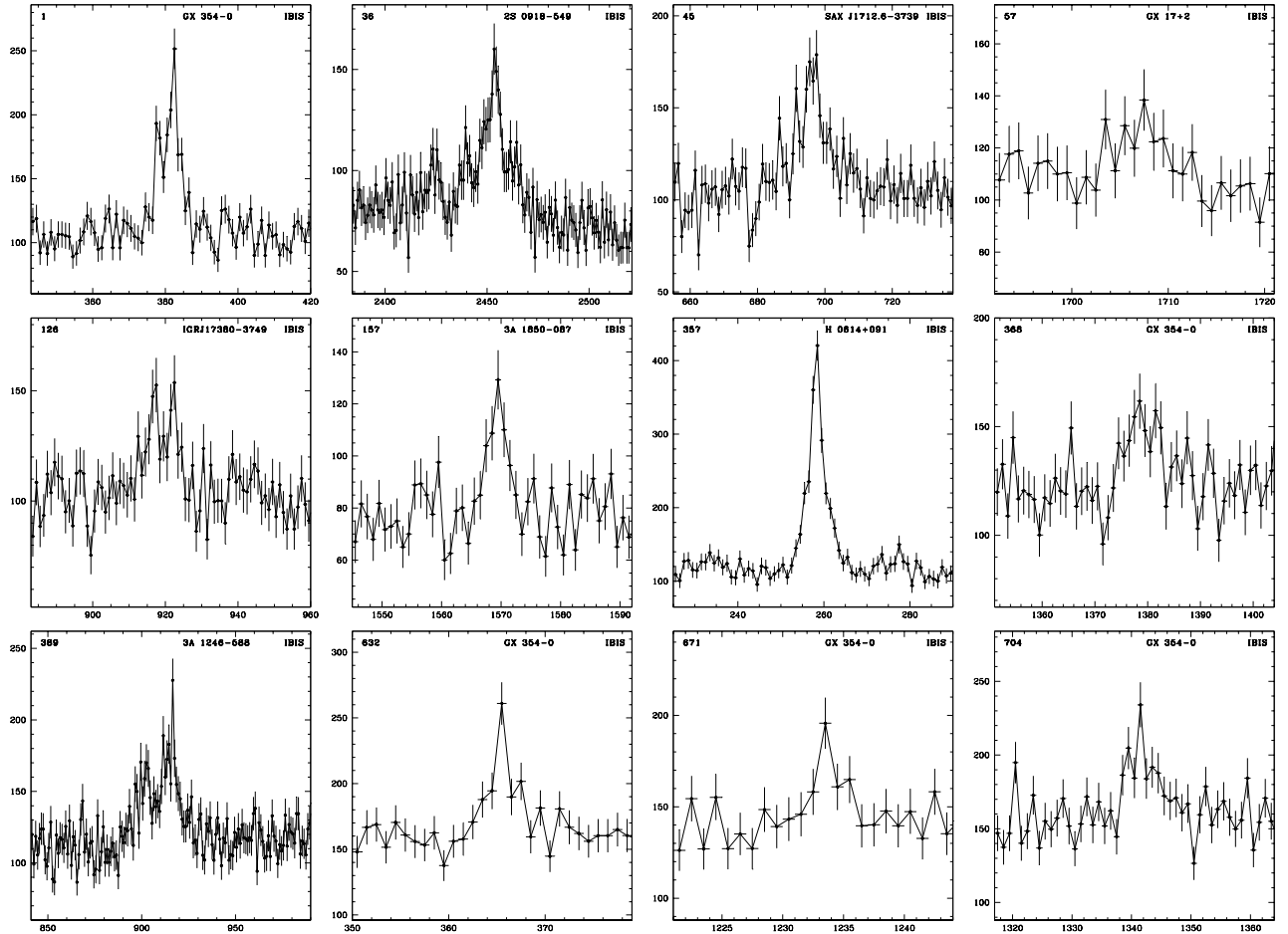


Fig. 3: Same as Fig. 2 but for the bursts that were recorded by IBIS at the edge of its field of view and that did not fall within the JEM-X field of view.

Table 1: X-ray bursts recorded by the IBIS/ISGRI telescope in the energy range 15-25 keV in 2003-2009

No.	Date	T_m^a	Source	T_{90}^b	F_m^c	T_e^d	T_{90}^j	F_m^j	T_e^j	No.	Date	T_m^a	Source	T_{90}^b	F_m^c	T_e^d	T_{90}^j	F_m^j	T_e^j
2003																			
1	Feb 28	07:55:07	GX 354-0	13	2.0	5.2				85	Sep 17	08:58:31	GX 354-0	7	2.5	4.0			
2	Mar 1	00:04:51	GX 354-0	11	2.4	4.9	30	5.6	10.4	86	Sep 17	15:12:20	GX 354-0	5	1.7	2.9			
3	Mar 1	16:05:33	GX 354-0	8	1.8	5.2				87	Sep 18	10:33:36	GX 354-0	8	1.4	3.6			
4	Mar 2	07:42:23	GX 354-0	9	2.0	5.4	20	5.7	9.0	88	Sep 19	16:12:10	GX 354-0	4	3.1	2.7	7	4.0	5.4
5	Mar 3	19:27:09	4U 1636-536	6	1.0	3.0				89	Sep 20	23:47:03	GX 354-0	10	1.9	5.7			
6	Mar 4	19:18:03	4U 1636-536	10	1.1	5.2	30	1.9	10.8	90	Sep 22	17:38:26	GX 354-0	5	2.1	2.7			
7	Mar 9	21:51:13	4U 1702-429	9	1.7	6.1				92	Sep 23	02:16:12	GX 354-0	6	1.7	4.3			
8	Mar 9	22:35:05	4U 1608-522	7	1.8	4.4				93	Sep 23	05:11:43	SLX 1735-269	9	1.0	4.8	11	4.0	6.9
9	Mar 11	06:01:49	4U 1702-429	3	2.3	2.2				94	Sep 23	10:53:37	GX 354-0	6	3.6	3.5			
10	Mar 12	10:22:26	GX 354-0	5	2.5	2.6				95	Sep 23	18:15:11	GX 354-0	7	1.9	3.8			
11	Mar 12	11:11:03	4U 1702-429	6	1.3	4.2				96	Sep 23	23:13:11	SLX 1735-269	8	0.8	5.7	21	1.9	8.4
12	Mar 13	13:49:36	4U 1608-522	10	1.9	5.3				97	Sep 24	03:52:12	GX 354-0	7	1.7	4.8			
13	Mar 15	02:38:00	4U 1702-429	8	1.5	5.1	26	4.1	9.4	98	Sep 24	11:01:28	GX 354-0	8	1.8	4.0			
14	Mar 15	12:01:33	GX 354-0	4	1.1	3.3				99	Sep 24	14:00:09	SAX J1712.6-3739	18	1.8	9.3			
15	Mar 15	15:45:08	GX 354-0	7	1.9	3.6				100	Sep 24	18:20:21	GX 354-0	5	1.6	3.2			
16	Mar 15	18:22:49	4U 1702-429	4	1.5	2.9				101	Sep 26	02:38:54	4U 1608-522	14	2.3	5.7			
17	Mar 15	20:36:46	GX 354-0	9	0.9	5.0				102	Sep 26	15:34:51	4U 1608-522	13	2.4	6.7			
18	Mar 16	00:53:36	GX 354-0	7	1.7	3.1				103	Sep 27	04:03:44	4U 1608-522	12	4.8	6.1	48	5.8	15.2
19	Mar 21	03:13:28	GX 354-0	6	1.8	3.8				104	Sep 27	16:08:45	4U 1812-12	17	2.2	7.8			
20	Mar 21	15:46:40	GX 354-0	5	1.4	3.1	14	3.6	4.7	105	Oct 2	05:20:46	4U 1608-522	14	2.2	7.0			
21	Mar 31	13:37:40	GX 354-0	9	1.4	6.8				106	Oct 3	01:56:32	GX 354-0	15	2.0	5.1			
22	Apr 3	08:40:18	GX 354-0	6	1.7	3.8				107	Oct 3	19:08:10	GX 354-0	5	2.4	3.1			
23	Apr 6	07:42:16	Aql X-1	10	1.2	5.3				108	Oct 4	11:22:25	GX 354-0	4	1.5	2.9			
24	Apr 6	18:32:30	4U 1724-307	12	1.2	6.8				109	Oct 4	16:08:04	GX 354-0	5	2.3	2.8			
25	Apr 6	19:45:29	GX 354-0	7	1.5	4.2	19	4.2	6.7	110	Oct 4	22:06:42	GX 354-0	8	1.1	4.3			
26	Apr 7	03:26:31	GX 354-0	8	1.4	4.2				111	Oct 5	09:34:42	GX 354-0	6	1.7	3.5			
27	Apr 9	22:36:23	Aql X-1	7	0.8	4.2				112	Oct 6	13:29:53	GX 354-0	6	2.1	3.2			
28	Apr 11	18:13:18	4U 1636-536	11	0.4	6.7				113	Oct 7	16:30:03	GX 354-0	7	1.2	4.0			
29	Apr 14	20:13:49	GX 354-0	5	1.3	3.6	15	2.6	6.3	114	Oct 7	21:53:01	GX 354-0	4	1.3	2.8			
30	Apr 15	00:30:22	GX 354-0	7	1.6	3.1	6	2.6	3.8	115	Oct 8	02:11:48	GX 354-0	6	2.0	3.4			
31	Apr 15	06:47:16	4U 1702-429	7	1.5	6.1				116	Oct 8	06:16:60	GX 354-0	5	1.0	3.0			
32	Apr 21	03:36:36	4U 1812-12	14	2.1	8.9				117	Oct 8	09:58:38	GX 354-0	5	1.4	3.4			
33	Apr 22	02:27:40	GX 354-0	5	0.9	3.5				118	Oct 8	13:48:29	GX 354-0	7	1.7	3.4			
34	Apr 22	06:15:00	GX 354-0	5	1.0	2.5	6	1.3	3.9	119	Oct 8	17:53:13	GX 354-0	5	2.2	3.2			
35	Apr 25	10:54:24	4U 1812-12	10	2.2	4.3				120	Oct 8	22:33:18	GX 354-0	3	2.0	2.6			
36	Jun 16	20:09:13	2S 0918-549	23	1.6	9.6				121	Oct 9	08:02:51	4U 1724-307	15	1.8	7.6			
37	Aug 9	06:30:25	4U 1636-536	7	0.9	4.4				122	Oct 10	16:50:48	SLX 1744-299	5	1.1	3.3			
38	Aug 18	10:05:10	4U 1702-429	7	1.8	4.7				123	Oct 18	00:12:16	4U 1812-12	18	4.0	4.3			
2004																			
40	Aug 19	11:02:36	GX 354-0	6	1.0	3.2				124	Feb 16	22:40:16	GX 354-0	6	2.0	4.0			
41	Aug 19	22:57:36	GX 354-0	3	1.5	2.5	21	2.3	7.0	125	Feb 17	04:47:52	GX 354-0	7	3.5	3.7			
42	Aug 23	16:14:02	GX 354-0	4	0.9	2.6	13	2.9	5.4	126	Feb 17	14:41:30	IGR J17380-3749	13	1.1	7.9			
43	Aug 23	21:06:35	GX 354-0	6	1.0	3.8				127	Feb 19	21:06:45	GX 354-0	6	2.0	3.7	16	5.2	6.5
44	Aug 24	22:20:44	GX 354-0	5	1.6	2.2				128	Feb 20	01:57:00	4U 1724-307	5	0.4	3.7	23	2.2	6.8
45	Aug 25	18:45:43	SAX J1712.6-3739	14	1.2	7.7				129	Feb 20	02:44:02	GX 354-0	8	1.7	4.8			
46	Aug 27	01:38:46	4U 1724-307	4	1.3	2.7				130	Feb 20	07:34:36	GX 354-0	5	2.1	3.0			
47	Aug 27	19:59:14	GX 354-0	7	1.3	4.5				131	Feb 20	12:00:24	GX 354-0	6	1.6	3.6			
48	Aug 28	01:24:04	GX 354-0	7	1.4	3.1	12	3.0	5.3	132	Feb 22	21:16:27	GX 354-0	6	1.7	3.2			
49	Aug 28	06:01:30	GX 354-0	6	1.3	4.1	12	2.6	4.6	133	Feb 27	08:51:11	GX 354-0	4	1.9	2.5			
50	Aug 29	14:31:29	GX 354-0	5	1.8	2.7				134	Feb 27	10:55:15	GX 354-0	6	2.7	3.2			
51	Aug 29	19:23:38	GX 354-0	5	1.4	3.6				135	Feb 27	13:32:37	GX 354-0	7	1.5	3.7	9	3.0	3.8
52	Aug 30	04:30:41	GX 354-0	5	1.0	3.3				136	Feb 27	15:32:03	GX 354-0	6	1.9	3.3	12	4.1	4.9
53	Aug 31	15:54:17	GX 354-0	7	0.8	4.4	12	3.1	5.1	137	Feb 28	13:46:45	GX 354-0	6	2.0	3.3	12	3.7	4.8
54	Sep 3	03:26:34	GX 354-0	5	1.0	3.9	13	4.0	5.9	138	Feb 28	16:57:36	GX 354-0	5	1.8	3.0			
55	Sep 3	08:39:32	GX 354-0	6	1.7	3.7	13	3.2	5.5	139	Mar 1	08:01:45	GX 354-0	7	1.1	5.3	13	3.7	5.6
56	Sep 3	18:02:39	GX 354-0	6	1.4	3.9				140	Mar 2	04:40:42	GX 354-0	5	1.2	2.9			
57	Sep 4	18:23:13	GX 17+2	5	1.0	2.3				141	Mar 2	05:50:12	4U 1724-307	6	0.7	4.1	24	3.1	8.2
58	Sep 6	00:23:44	4U 1812-12	10	2.6	4.1				142	Mar 2	07:34:39	GX 354-0	7	1.3	3.6			
59	Sep 7	20:30:07	GX 354-0	5	1.1	2.8				143	Mar 2	09:25:34	GX 3+1	5	0.9	2.9	11	2.4	5.9
60	Sep 8	13:41:35	GX 354-0	5	1.8	2.9				144	Mar 2	16:37:23	GX 354-0	3	1.2	1.9			
61	Sep 8	18:48:29	4U 1724-307	44	1.6	20.7	98	2.8	64.2	145	Mar 2	17:24:15	4U 1724-307	9	1.3	3.7			
62	Sep 8	19:41:20	GX 354-0	5	2.1	3.6	14	5.0	5.8	146	Mar 3	02:51:12	GX 354-0	5	1.2	2.9			
63	Sep 9	03:11:36	GX 354-0	6	3.2	3.2				147	Mar 3	04:14:60	4U 1724-307	9	1.1	5.1	26	2.6	9.0
64	Sep 9	10:02:43	GX 354-0	11	2.3	5.0				148	Mar 3	05:44:13	4U 1812-12	8	1.5	4.6			
65	Sep 9	16:28:54	GX 354-0	7	1.5	3.4</													

Table 1: Contd.

No.	Date	T_m^a	Source	T_{90}^b	F_m^c	T_e^d	T_{90}^j	F_m^j	T_e^j	No.	Date	T_m^a	Source	T_{90}^b	F_m^c	T_e^d	T_{90}^j	F_m^j	T_e^j
169	Mar 30	03:37:46	SLX 1744-299	22	1.2	10.6				254	Oct 1	07:37:39	4U 1724-307	6	1.1	3.5	52	3.0	20.7
170	Mar 30	03:43:45	KS 1741-293	7	0.5	4.3				255	Oct 1	14:28:34	GX 354-0	5	1.9	3.6			
171	Mar 30	10:38:17	KS 1741-293	7	0.9	3.6	10	0.6	4.9	256	Oct 1	22:11:34	GX 354-0	4	2.0	2.8			
172	Mar 30	18:35:54	GX 354-0	6	1.8	3.8				257	Oct 2	01:58:58	GX 354-0	7	2.1	4.1			
173	Mar 31	03:08:58	GX 354-0	6	0.9	3.6	8	6.3	3.5	258	Oct 2	05:59:15	GX 354-0	6	2.2	3.7	14	5.1	5.6
174	Mar 31	10:27:26	GX 354-0	5	1.0	3.7				259	Oct 2	10:12:10	GX 354-0	6	1.8	3.5			
175	Apr 1	23:36:52	GX 354-0	5	1.2	3.1				260	Oct 2	14:16:06	GX 354-0	5	2.1	4.1			
176	Apr 2	01:41:40	GX 354-0	3	1.4	2.4	9	2.7	4.6	261	Oct 2	18:27:58	GX 354-0	5	1.6	3.9			
177	Apr 2	07:19:37	GX 354-0	4	0.8	3.3	10	2.0	5.5	262	Oct 2	21:50:09	GX 354-0	8	1.7	4.4	13	5.0	5.5
178	Apr 8	08:12:41	GX 354-0	4	1.3	2.5				263	Oct 4	03:15:49	4U 1812-12	16	2.4	6.8			
179	Apr 8	15:07:02	GX 354-0	6	0.9	4.3				264	Oct 4	09:02:16	GX 354-0	9	2.1	3.9			
180	Apr 8	18:56:50	GX 354-0	6	1.6	3.7				265	Oct 4	12:29:39	GX 354-0	6	1.9	3.5	13	6.3	5.5
181	Apr 13	11:24:19	GX 354-0	6	2.0	3.7				266	Oct 4	15:08:42	GX 354-0	4	1.2	2.7			
182	Apr 14	00:30:57	GX 354-0	7	2.6	4.1				267	Oct 4	17:46:24	GX 354-0	4	2.5	2.7			
183	Apr 14	08:27:03	GX 354-0	4	2.4	2.4				268	Oct 4	23:42:01	GX 354-0	4	2.3	3.0			
184	Apr 19	19:18:59	GX 354-0	7	1.7	3.5				269	Oct 5	04:57:10	GX 354-0	6	3.2	3.3	17	4.2	5.4
185	Apr 20	03:06:43	GX 354-0	8	1.7	4.1				270	Oct 5	07:45:01	GX 354-0	5	2.0	3.1			
186	Apr 20	17:24:01	XB 1832-330	11	1.1	5.9				271	Oct 5	09:58:21	GX 354-0	4	2.0	2.5			
187	Apr 28	07:54:46	Aql X-1	7	1.4	3.4				272	Oct 5	12:12:41	GX 354-0	5	2.7	3.1			
188	Apr 29	21:47:41	3A 1850-087	10	1.2	7.3				273	Oct 5	14:47:45	GX 354-0	7	1.5	3.6			
189	May 1	22:56:43	Aql X-1	10	1.4	4.1	41	4.0	15.3	274	Oct 5	17:11:14	GX 354-0	4	1.4	3.0			
190	Aug 16	02:16:06	4U 1702-429	5	0.7	3.6				275	Oct 5	21:38:01	GX 354-0	5	3.4	2.3			
191	Aug 21	21:19:52	GX 354-0	5	1.3	2.2				276	Oct 9	12:14:17	GX 354-0	4	2.5	2.2			
192	Aug 22	14:37:53	GX 354-0	7	1.4	3.6	12	5.6	6.4	277	Oct 11	12:59:12	GX 354-0	6	2.4	3.2	14	4.6	5.3
193	Aug 22	18:02:05	GX 354-0	8	2.0	3.2				278	Oct 11	23:10:50	GX 354-0	4	2.1	3.0			
194	Aug 22	23:40:11	GX 354-0	13	0.9	5.4				279	Oct 12	19:42:57	GX 354-0	4	1.9	2.8			
195	Aug 23	00:11:52	4U 1724-307	6	0.8	3.8	11	2.5	5.0	280	Oct 16	00:01:07	GX 354-0	4	1.3	2.7	14	2.7	5.9
196	Aug 23	02:16:08	GX 354-0	6	2.1	3.3				281	Oct 16	07:27:17	GX 354-0	4	1.3	3.1	12	2.9	5.1
197	Aug 23	10:06:32	GX 354-0	6	0.7	3.4				282	Oct 17	10:58:54	GX 354-0	7	1.3	3.5	15	3.2	5.1
198	Aug 23	16:12:18	GX 354-0	9	0.7	4.5				283	Oct 17	14:10:29	GX 354-0	5	0.9	3.2			
199	Aug 23	17:23:59	SLX 1735-269	27	1.7	15.9	160	4.1	97.9	284	Oct 19	21:34:24	GX 354-0	3	1.3	2.2			
200	Aug 23	21:53:59	GX 354-0	7	1.6	3.3				285	Oct 20	06:37:13	GX 354-0	6	1.2	3.5	16	3.7	4.9
201	Aug 24	06:24:27	GX 354-0	5	1.2	3.1	13	3.4	5.6	286	Oct 20	11:35:45	GX 354-0	6	1.2	3.4			
202	Aug 24	13:05:21	4U 1636-536	4	1.1	2.8													
203	Aug 28	21:17:04	4U 1702-429	7	1.5	3.2				287	Feb 6	19:07:47	4U 1636-536	5	0.7	3.1			
204	Aug 30	15:57:27	4U 1724-307	5	1.4	3.1	28	2.6	13.6	288	Feb 7	06:33:39	4U 1702-429	6	2.1	2.9			
205	Sep 1	01:22:21	GX 354-0	6	0.9	3.0				289	Feb 14	11:50:16	4U 1702-429	9	0.5	6.4			
206	Sep 1	15:25:02	GX 354-0	5	1.2	2.9				290	Feb 16	05:56:52	GX 354-0	4	1.4	3.3			
207	Sep 1	19:26:43	GX 354-0	5	1.8	3.6	12	3.4	4.5	291	Feb 16	09:29:20	GX 354-0	5	2.7	3.6	15	4.2	5.3
208	Sep 1	23:12:18	GX 354-0	6	1.2	3.9	8	4.4	4.4	292	Feb 16	13:54:53	GX 354-0	6	3.1	3.4	21	4.5	6.7
209	Sep 2	02:32:25	GX 354-0	7	1.3	3.0				293	Feb 16	17:19:47	GX 354-0	8	2.9	3.4			
210	Sep 2	07:16:21	GX 354-0	7	1.4	3.8				294	Feb 16	19:49:26	4U 1724-307	9	1.1	6.4	62	3.5	23.0
211	Sep 2	18:30:48	GX 354-0	5	1.3	3.3				295	Feb 16	20:41:03	GX 354-0	5	3.2	3.5			
212	Sep 2	22:37:42	GX 354-0	7	0.9	4.5				296	Feb 17	03:35:27	GX 354-0	4	3.3	3.3			
213	Sep 3	14:32:30	GX 354-0	4	1.3	2.5				297	Feb 17	06:58:45	GX 354-0	6	2.5	4.1			
214	Sep 3	18:39:35	GX 354-0	8	1.3	4.0				298	Feb 17	10:51:19	GX 354-0	4	4.3	2.3	9	5.0	5.2
215	Sep 3	20:00:53	4U 1724-307	13	0.8	5.1				299	Feb 18	15:35:56	4U 1702-429	8	1.0	4.4			
216	Sep 3	23:17:42	GX 354-0	8	1.8	3.6				300	Feb 19	02:26:13	4U 1702-429	8	1.5	5.6			
217	Sep 4	04:15:09	GX 354-0	5	3.2	3.0				301	Feb 19	03:00:58	4U 1636-536	6	1.7	4.2			
218	Sep 4	09:06:02	GX 354-0	4	1.6	2.5				302	Feb 19	14:27:24	4U 1702-429	6	2.4	3.9			
219	Sep 4	16:19:11	GX 354-0	6	1.3	4.1				303	Feb 19	15:38:52	4U 1636-536	5	1.9	2.9	17	3.3	5.9
220	Sep 4	23:50:04	GX 354-0	3	1.9	2.9				304	Feb 21	10:06:19	GX 354-0	4	1.6	3.1			
221	Sep 7	10:51:47	4U 1702-429	5	1.5	3.2	13	4.3	5.9	305	Feb 21	18:50:30	4U 1636-536	3	1.5	2.0			
222	Sep 7	11:09:51	GX 354-0	4	0.9	3.1				306	Feb 22	12:33:07	4U 1702-429	6	1.6	4.3			
223	Sep 7	14:27:14	GX 354-0	4	2.1	3.0				307	Feb 22	13:49:00	4U 1636-536	9	1.1	4.9			
224	Sep 7	18:04:56	GX 354-0	5	1.0	4.3				308	Feb 22	23:01:00	4U 1636-536	5	1.1	3.6			
225	Sep 7	21:30:48	GX 354-0	5	1.6	3.5	16	4.1	5.7	309	Feb 24	10:56:05	4U 1702-429	7	1.6	3.8			
226	Sep 7	23:29:56	4U 1724-307	9	1.2	4.1	30	1.9	14.4	310	Feb 24	20:22:07	4U 1702-429	10	0.8	5.7	17	3.2	6.6
227	Sep 8	01:54:26	GX 354-0	7	1.5	3.4				311	Feb 25	04:53:55	4U 1702-429	6	1.1	3.4			
228	Sep 8	05:39:23	GX 354-0	3	2.7	2.4				312	Feb 25	13:58:35	4U 1702-429	6	2.0	3.5			
229	Sep 8	09:00:22	GX 354-0	5	1.3	3.3				313	Feb 26	10:30:35	4U 1702-429	9	1.5	5.3			
230	Sep 8	12:41:39	GX 354-0	5	1.1	3.5	15	3.9	5.1	314	Feb 27	16:08:41	4U 1702-429	10	2.3	4.8			
231	Sep 8	15:50:10	GX 354-0	8	1.7	2.9				315	Mar 3	19:46:16	4U 1608-522	11	3.5	4.8			
232	Sep 8	17:43:26	4U 1702-429	5	0.9	3.4				316	Mar 4	13:16:30	4U 1608-522	9	2.2	5.9			
233	Sep 10	01:05:38	4U 1702-429	7	1.1	3.7				317	Mar 5	22:37:27	4U 1608-522	17	2.6	7.8			
234	Sep 11	04:16:54	4U 1636-536	8	1.1	4.0	23	2.7	7.2	318									

Table 1: Contd.

No.	Date	T_m^a	Source	T_{90}^b	F_m^c	T_e^d	T_{90}^j	F_m^j	T_e^j	No.	Date	T_m^a	Source	T_{90}^b	F_m^c	T_e^d	T_{90}^j	F_m^j	T_e^j
338	Mar 21	03:40:50	GX 354-0	4	1.4	2.0				423	Sep 23	10:36:04	GX 354-0	6	1.9	3.4			
339	Mar 21	09:09:51	4U 1724-307	9	1.4	4.9				424	Sep 24	20:25:07	GX 354-0	7	2.5	4.4			
340	Mar 21	19:06:06	SAX J1712.6-3739	17	1.6	11.8				425	Sep 25	12:15:47	GX 354-0	5	1.2	2.4			
341	Mar 22	01:24:37	GX 354-0	6	1.7	2.6				426	Sep 25	14:55:49	GX 354-0	5	1.5	3.1			
342	Mar 22	23:59:45	GX 354-0	6	2.4	3.6				427	Sep 26	20:29:29	GX 354-0	4	1.8	2.5			
343	Mar 23	11:44:33	GX 354-0	6	1.5	3.4				428	Sep 29	01:13:48	GX 354-0	5	1.0	3.0			
344	Mar 23	16:51:10	GX 354-0	4	2.2	2.8	10	2.5	4.9	429	Sep 29	04:31:10	4U 1724-307	4	1.3	2.7			
345	Mar 24	15:39:10	GX 354-0	5	1.2	3.3	21	3.7	6.2	430	Sep 29	10:22:29	GX 354-0	4	2.0	2.5			
346	Mar 24	21:14:22	GX 354-0	6	2.0	4.1				431	Sep 30	14:26:24	4U 1724-307	4	0.7	3.2			
347	Mar 25	02:22:48	GX 354-0	5	1.7	3.4				432	Oct 1	04:30:05	4U 1724-307	5	1.2	2.7			
348	Mar 25	06:12:24	GX 354-0	4	2.3	2.5				433	Oct 1	21:51:29	GX 354-0	11	1.1	6.2	11	3.5	4.5
349	Mar 25	23:51:29	GX 354-0	5	1.8	3.4				434	Oct 2	01:37:34	GX 354-0	11	1.3	4.6	20	3.5	6.6
350	Mar 26	04:00:54	GX 354-0	5	3.4	2.9				435	Oct 2	02:14:09	4U 1724-307	5	1.1	3.0	41	0.4	11.5
351	Mar 26	09:05:20	GX 354-0	8	2.6	3.7				436	Oct 2	05:33:56	GX 354-0	5	2.6	3.5	13	4.0	5.6
352	Mar 27	08:45:39	GX 354-0	6	1.3	4.5				437	Oct 2	09:13:39	GX 354-0	7	1.2	3.9	10	2.1	6.2
353	Mar 27	11:49:04	4U 1702-429	9	1.2	4.8				438	Oct 4	04:49:37	4U 1724-307	7	0.9	4.5			
354	Mar 27	15:23:04	GX 354-0	5	2.6	3.0				439	Oct 6	09:10:25	4U 1724-307	7	1.0	5.2			
355	Mar 27	20:07:35	4U 1702-429	17	0.8	8.7	25	3.4	8.6	440	Oct 6	13:46:01	GX 354-0	10	1.5	4.9			
356	Mar 28	01:47:04	GX 354-0	6	2.1	3.6				441	Oct 6	18:17:39	GX 354-0	7	2.0	3.1			
357	Mar 31	07:13:08	H 0614+091	11	5.2	4.2				442	Oct 6	22:45:55	GX 354-0	9	2.1	3.9			
358	Apr 2	03:28:57	GX 354-0	4	1.4	2.4				443	Oct 7	03:04:10	GX 354-0	5	1.3	3.5			
359	Apr 4	01:17:29	GX 354-0	4	2.0	2.6				444	Oct 7	03:42:27	4U 1724-307	8	1.8	4.1			
360	Apr 4	04:55:51	4U 1702-429	6	2.1	3.4				445	Oct 7	11:10:31	GX 354-0	6	2.1	4.0	17	3.4	5.5
361	Apr 6	04:53:50	4U 1636-536	8	1.2	4.4				446	Oct 7	15:29:33	GX 354-0	5	3.3	3.5	20	5.1	6.1
362	Apr 6	08:56:54	4U 1702-429	15	1.8	6.8				447	Oct 7	22:36:56	GX 354-0	4	1.2	2.6			
363	Apr 7	10:06:45	GX 354-0	4	1.0	2.7				448	Oct 9	17:04:38	4U 1812-12	6	2.3	3.5			
364	Apr 8	06:04:19	4U 1702-429	17	1.6	7.4				449	Oct 12	11:04:10	IA 1743-288	7	1.0	5.0	18	0.7	8.9
365	Apr 8	17:27:27	4U 1636-536	5	2.4	3.3	17	3.0	5.8	450	Oct 15	15:28:21	4U 1608-522	7	2.1	3.6			
366	Apr 9	07:58:01	GX 354-0	6	1.6	2.9	9	4.2	4.3	451	Oct 25	20:24:19	4U 1812-12	20	2.8	6.4	58	5.4	21.3
367	Apr 10	03:01:03	4U 1702-429	9	3.0	5.9	19	4.7	9.3	452	Oct 26	15:27:43	GX 354-0	5	1.3	3.5			
368	Apr 10	07:42:24	GX 354-0	9	1.7	4.8				453	Nov 9	00:40:16	2S 0918-549	5	1.1	3.7			
2006																			
370	Apr 11	08:15:60	SLX 1737-282	230	2.1	103.5	83	4.0	42.2	454	Feb 14	22:31:13	GX 354-0	5	1.1	3.5			
371	Apr 11	15:52:58	GX 354-0	8	2.7	4.3	12	3.2	5.4	455	Feb 16	21:53:60	XB 1832-330	7	0.8	4.3	32	1.3	12.3
372	Apr 14	06:33:29	GX 354-0	3	1.8	2.3				456	Feb 18	03:47:27	GX 354-0	7	1.5	4.4			
373	Apr 14	17:03:34	GX 354-0	5	1.0	4.0	16	3.0	5.6	457	Feb 18	09:22:32	GX 354-0	7	1.3	3.9	17	2.3	5.9
374	Apr 14	21:50:02	4U 1724-307	9	2.0	5.4	31	3.4	17.3	458	Feb 18	13:55:45	GX 354-0	5	1.9	2.4	11	3.0	3.8
375	Apr 16	07:02:19	GX 354-0	6	1.6	3.8				459	Feb 19	12:03:49	GX 354-0	3	1.3	2.8			
376	Apr 16	17:15:49	GX 354-0	4	1.7	2.5				460	Feb 19	19:57:35	GX 354-0	7	1.2	3.8	16	2.6	5.9
377	Apr 16	22:11:04	AX J1754.2-2754	46	1.8	23.5	76	3.4	39.3	461	Feb 20	21:28:10	GX 354-0	4	1.3	2.6			
378	Apr 16	22:17:44	4U 1724-307	9	1.0	4.5				462	Feb 20	23:34:45	GX 354-0	6	1.1	3.2			
379	Apr 17	11:31:20	GX 354-0	6	1.6	3.7	11	2.6	6.0	463	Feb 24	09:53:43	4U 1724-307	3	1.8	2.1	22	2.6	9.2
380	Apr 17	13:49:26	GX 354-0	5	1.0	3.8	12	1.6	5.4	464	Feb 25	09:58:13	GX 354-0	5	1.8	3.4	8	3.1	4.1
381	Apr 17	18:13:55	GX 354-0	6	1.7	3.4	13	4.2	5.0	465	Feb 25	17:13:31	GX 354-0	4	1.5	3.1	14	3.8	4.3
382	Apr 17	21:38:48	GX 354-0	4	1.1	2.5				466	Feb 28	19:14:37	GX 354-0	6	1.9	3.0	10	3.6	4.4
383	Apr 19	16:16:04	4U 1724-307	13	2.1	4.6	31	3.7	12.5	467	Mar 2	21:30:41	GX 354-0	4	1.5	2.8			
384	Apr 19	16:56:22	GX 354-0	5	0.9	3.7	15	3.9	5.5	468	Mar 3	00:36:25	GX 354-0	5	1.3	3.9	14	0.3	5.6
385	Apr 20	00:38:39	GX 354-0	7	1.9	3.6				469	Mar 3	15:31:49	4U 1812-12	4	3.5	2.6			
386	Apr 21	00:48:39	GX 354-0	5	1.7	3.0	15	3.8	5.2	470	Mar 4	05:18:10	GX 354-0	6	1.7	4.0			
387	Apr 21	03:37:02	4U 1724-307	7	0.9	5.2				471	Mar 4	06:31:56	4U 1724-307	6	1.3	3.0			
388	Apr 28	06:00:38	4U 1812-12	12	4.1	3.9	58	7.8	20.9	472	Mar 4	08:18:41	GX 354-0	6	1.1	3.5			
389	Jun 27	11:06:54	3A 1246-588	25	6.2	9.4				473	Mar 6	04:59:14	GX 354-0	4	2.1	2.7			
390	Aug 11	14:06:28	4U 1812-12	6	3.8	3.0				474	Mar 6	08:13:15	GX 354-0	4	1.4	2.5			
391	Aug 12	16:47:26	GX 354-0	6	1.3	3.2				475	Mar 6	11:31:36	GX 354-0	6	1.5	3.3			
392	Aug 12	22:09:58	4U 1608-522	5	2.6	2.8				476	Mar 6	15:29:35	GX 354-0	7	1.8	3.9			
393	Aug 17	03:06:31	GX 354-0	5	2.2	3.8				477	Mar 6	19:36:33	GX 354-0	5	1.8	2.6			
394	Aug 17	08:55:27	4U 1608-522	4	5.3	2.7				478	Mar 8	04:27:09	GX 354-0	6	1.4	3.1	16	2.6	5.3
395	Aug 25	16:19:39	GX 354-0	6	1.5	3.9				479	Mar 8	02:45:44	GX 354-0	5	2.1	3.1			
396	Aug 25	21:28:22	4U 1636-536	7	1.3	4.7				480	Mar 9	02:31:37	GX 354-0	4	1.0	3.2			
397	Aug 26	07:07:35	4U 1702-429	5	1.5	3.4				481	Mar 9	09:13:56	GX 354-0	4	2.4	2.2			
398	Aug 26	10:51:25	4U 1608-522	14	3.4	6.7				482	Mar 9	12:33:18	GX 354-0	6	1.5	4.1			
399	Aug 27	11:34:03	4U 1608-522	17	3.1	5.8	41	7.4	12.7	483	Mar 9	16:13:25	GX 354-0	5	1.6	3.5			
400	Aug 28	13:24:16	GX 354-0	4	4.0	2.3				484	Mar 10	19:40:29	GX 354-0	5	2.3	3.2	11	3.8	4.7
401	Aug 28	21:39:42	GX 354-0	6	4.1	4.1				485	Mar 10	22:42:46	GX 354-0	8	2.0	3.9	26	4.1	5.8
402	Aug 29	08:29:35	GX 354-0	7	4.0	3.6	</												

Table 1: Contd.

No.	Date	T_m^a	Source	T_{90}^b	F_m^c	T_e^d	T_{90}^j	F_m^j	T_e^j	No.	Date	T_m^a	Source	T_{90}^b	F_m^c	T_e^d	T_{90}^j	F_m^j	T_e^j
507	Mar 28	04:04:41	GX 354-0	5	1.4	3.5				592	Sep 9	12:34:22	4U 1724-307	14	2.1	4.9	45	4.4	23.7
508	Mar 28	07:24:43	GX 354-0	7	2.2	2.9				593	Sep 9	14:13:13	GX 354-0	8	2.4	3.7			
509	Apr 1	03:37:59	GX 354-0	6	1.2	4.1				594	Sep 12	11:20:03	GX 354-0	4	1.7	2.6			
510	Apr 3	19:29:21	GX 354-0	6	1.9	3.4				595	Sep 13	14:18:01	GX 354-0	6	1.3	3.6	10	4.0	4.2
511	Apr 4	01:37:48	4U 1724-307	8	2.0	3.8				596	Sep 13	18:22:51	GX 354-0	6	1.8	4.0	12	4.5	5.1
512	Apr 4	05:14:00	GX 354-0	4	1.9	2.8				597	Sep 13	23:15:35	GX 354-0	5	2.7	3.2	17	3.3	5.7
513	Apr 4	17:39:06	GX 354-0	6	0.8	3.5				598	Sep 14	03:12:05	GX 354-0	7	1.6	3.9	9	3.9	4.2
514	Apr 4	21:19:38	4U 1724-307	4	1.5	2.9				599	Sep 15	09:04:43	GX 354-0	5	1.0	3.3			
515	Apr 5	02:46:33	GX 354-0	5	2.3	3.2	12	1.1	4.1	600	Sep 15	19:59:39	GX 354-0	6	1.9	3.0			
516	Apr 5	04:54:40	GX 354-0	7	2.0	3.3	20	3.5	5.1	601	Sep 15	23:06:26	GX 354-0	4	2.2	2.8	16	5.4	4.4
517	Apr 5	13:30:25	GX 354-0	5	1.9	3.4	13	3.0	4.8	602	Sep 16	06:41:29	GX 354-0	5	3.8	3.2	8	3.8	4.1
518	Apr 5	19:40:10	4U 1724-307	7	0.5	5.1				603	Sep 16	10:52:42	GX 354-0	4	3.1	2.8			
519	Apr 5	21:22:04	GX 354-0	4	1.7	2.9				604	Sep 16	14:12:56	GX 354-0	6	2.7	3.4			
520	Apr 7	12:33:18	GX 354-0	7	0.5	4.1				605	Sep 16	21:16:32	GX 354-0	6	1.4	4.1			
521	Apr 8	06:31:37	GX 354-0	5	2.5	3.6	20	4.5	5.1	606	Sep 17	09:59:43	GX 354-0	4	3.1	2.5			
522	Apr 8	14:21:05	GX 354-0	4	1.5	3.0				607	Sep 17	13:38:49	GX 354-0	5	2.6	3.7			
523	Apr 10	01:54:24	XB 1832-330	7	1.2	4.3				608	Sep 18	08:49:27	GX 354-0	10	2.6	4.8			
524	Apr 10	13:16:22	GX 354-0	5	1.0	3.5	13	3.2	5.0	609	Sep 18	12:04:18	GX 354-0	4	2.7	2.7			
525	Apr 10	20:23:22	GX 354-0	6	1.3	3.9				610	Sep 18	15:53:14	GX 354-0	5	2.8	3.1	20	4.9	6.0
526	Apr 10	22:50:40	GX 354-0	5	1.2	3.3	18	3.8	5.8	611	Sep 18	18:40:07	GX 354-0	5	2.8	3.4	13	3.7	4.3
527	Apr 11	04:52:35	4U 1724-307	6	1.7	2.4				612	Sep 18	20:57:48	4U 1724-307	6	1.2	4.3			
528	Apr 11	11:45:40	GX 354-0	5	1.4	3.8				613	Sep 18	22:14:47	GX 354-0	7	1.7	4.2			
529	Apr 11	17:55:55	GX 354-0	5	1.2	3.2				614	Sep 18	23:49:57	SLX 1737-282	370	1.5	111.6			
530	Apr 12	17:09:18	GX 354-0	6	1.8	4.0				615	Sep 20	00:21:43	GX 354-0	3	3.1	2.2	14	3.4	5.0
531	Apr 13	01:00:35	GX 354-0	6	1.5	3.0	12	3.9	5.2	616	Sep 20	03:29:34	GX 354-0	5	3.9	3.2	15	4.6	5.8
532	Apr 13	03:38:19	GX 354-0	6	1.5	2.9	16	2.4	5.5	617	Sep 20	06:24:34	GX 354-0	4	1.5	2.9			
533	Apr 13	09:38:20	4U 1724-307	11	1.1	5.5	44	2.8	21.4	618	Sep 20	09:14:48	GX 354-0	4	2.8	3.2			
534	Apr 13	10:18:57	GX 354-0	8	1.3	4.9	13	3.8	4.8	619	Sep 20	12:20:00	GX 354-0	11	2.3	4.9			
535	Apr 13	13:31:42	GX 354-0	5	1.1	4.0	12	4.2	5.0	620	Sep 21	04:58:19	GX 354-0	5	3.5	3.7			
536	Apr 13	17:13:58	GX 354-0	4	0.5	3.3				621	Sep 21	08:14:00	GX 354-0	6	2.1	3.8			
537	Apr 13	22:40:15	GX 354-0	8	1.2	3.4	11	2.5	5.1	622	Sep 21	10:33:06	GX 354-0	5	0.7	2.1			
538	Apr 14	07:36:31	GX 354-0	4	2.0	2.4				623	Sep 22	05:41:44	GX 354-0	4	4.6	3.0			
539	Apr 14	18:17:58	1A 1743-288	4	2.0	2.3	11	2.7	7.5	624	Sep 22	08:00:45	GX 354-0	5	3.4	3.2	9	4.4	4.9
540	Apr 15	16:03:22	GX 354-0	3	2.7	2.2				625	Sep 22	10:44:42	GX 354-0	6	2.3	3.2			
541	Apr 15	18:11:60	4U 1724-307	8	1.1	4.2				626	Sep 22	13:16:55	GX 354-0	7	4.6	3.1	12	3.1	4.6
542	Apr 15	18:52:58	GX 354-0	8	0.9	3.7				627	Sep 22	15:28:21	GX 354-0	7	3.3	3.8	19	4.9	5.3
543	Apr 16	11:10:44	GX 354-0	6	1.9	2.7				628	Sep 22	18:01:46	GX 354-0	9	3.0	4.2	23	6.4	6.6
544	Apr 16	16:10:43	GX 354-0	13	1.4	5.3				629	Sep 22	20:15:35	GX 354-0	4	2.2	2.8			
545	Apr 16	23:14:47	GX 354-0	8	1.7	4.7	16	3.0	6.0	630	Sep 22	23:20:00	GX 354-0	6	2.2	4.1			
546	Apr 17	03:03:19	GX 354-0	4	1.6	3.1				631	Sep 24	02:32:31	GX 354-0	5	2.2	3.2			
547	Apr 17	09:24:26	GX 354-0	7	1.7	3.4	19	3.7	5.1	632	Sep 26	13:11:55	GX 354-0	5	2.2	2.3			
548	Apr 19	15:33:06	4U 1812-12	18	2.9	6.1				633	Sep 30	11:08:23	GX 354-0	8	1.3	5.1	9	1.7	4.6
549	Apr 21	02:24:09	GX 354-0	6	2.3	3.4				634	Oct 1	09:17:14	GX 354-0	7	0.7	4.5	13	3.7	4.5
550	Apr 25	20:55:15	4U 1812-12	18	2.9	5.5	58	9.0	19.1	635	Oct 1	14:20:18	GX 354-0	5	2.4	2.8	10	2.7	3.7
551	May 19	21:20:60	2S 0918-549	9	2.5	4.2				636	Sep 30	14:17:19	4U 1702-429	8	2.6	3.8			
552	Aug 14	17:06:22	4U 1702-429	13	1.6	6.5	23	3.9	11.9	637	Sep 3	15:33:43	GX 354-0	4	1.7	2.7	10	0.4	4.7
553	Aug 16	07:15:19	4U 1724-307	6	1.3	4.6	18	2.9	7.5	638	Sep 5	02:40:54	GX 354-0	5	1.0	3.6	13	3.6	5.5
554	Aug 19	04:38:43	GX 354-0	5	1.5	3.4				639	Sep 17	02:55:33	GX 354-0	4	2.4	3.0			
555	Aug 25	22:59:34	GX 354-0	5	1.5	2.8				640	Sep 24	02:15:45	4U 1724-307	5	1.0	3.0			
556	Aug 26	02:48:41	GX 354-0	4	2.1	3.0				641	Jan 31	08:01:48	4U 1702-429	6	1.0	3.5			
557	Aug 26	07:05:35	GX 354-0	6	2.0	3.6				642	Feb 1	05:25:47	4U 1702-429	7	1.9	4.2	17	3.7	8.4
558	Aug 26	15:44:27	GX 354-0	5	1.2	3.9				643	Feb 15	19:22:39	4U 1724-307	12	1.4	6.8	70	2.6	12.6
559	Aug 26	19:53:25	GX 354-0	5	3.4	2.9	19	4.3	5.9	644	Feb 15	20:02:00	GX 354-0	4	1.7	3.3			
560	Aug 26	23:24:06	GX 354-0	7	2.5	3.5				645	Feb 15	22:11:44	GX 354-0	6	2.4	3.4			
561	Aug 26	23:33:28	4U 1724-307	7	1.3	3.7				646	Feb 18	02:30:38	4U 1702-429	10	2.0	6.1	26	3.4	12.8
562	Aug 27	06:28:22	GX 354-0	5	1.6	3.7				647	Feb 18	14:13:07	4U 1702-429	6	3.4	3.2			
563	Aug 27	17:34:50	GX 354-0	5	1.2	3.1				648	Feb 19	04:22:26	4U 1702-429	7	1.3	4.0			
564	Aug 28	08:32:50	GX 354-0	4	1.3	2.3				649	Feb 27	10:36:21	GX 354-0	4	1.4	2.6			
565	Aug 28	13:01:43	GX 354-0	8	1.3	5.1				650	Feb 27	21:46:09	4U 1812-12	17	2.3	7.2			
566	Aug 28	16:59:16	GX 354-0	6	1.9	3.7	15	3.7	4.5	651	Feb 28	08:57:01	GX 354-0	6	2.5	2.9			
567	Aug 28	20:37:25	GX 354-0	4	1.8	2.8				652	Feb 28	13:57:11	GX 354-0	7	1.9	4.1	18	4.1	5.0
568	Aug 29	11:08:26	GX 354-0	4	2.1	2.6				653	Feb 28	18:43:48	GX 354-0	7	1.6	3.2	14	4.7	5.4
569	Aug 29	14:58:35	GX 354-0	5	1.6	3.3				654	Feb 28	23:50:10	GX 354-0	3	1.5	2.0			
570	Aug 29	22:39:19	GX 354-0	5	1.7	3.0				655	Mar 1	03:14:21	4U 1702-429	8	1.9	5.5	12	4.9	7.3
571	Aug 30	01:49:32	GX 354-0	3	2.1	2.2													

Table 1: Contd.

No.	Date	T_m^a	Source	T_{90}^b	F_m^c	T_e^d	T_{90}^j	F_m^j	T_e^j	No.	Date	T_m^a	Source	T_{90}^b	F_m^c	T_e^d	T_{90}^j	F_m^j	T_e^j
676	Mar 9	07:00:00	GX 354-0	5	1.9	3.6				757	Oct 15 2008	01:42:18	SAX J1810.8-2609	12	2.8	6.2			
677	Mar 9	10:30:33	GX 354-0	5	2.2	4.0				758	Feb 24	20:03:27	4U 1812-12	8	2.7	3.4			
678	Mar 9	14:09:02	GX 354-0	6	2.5	3.2				759	Mar 3	23:31:10	4U 1812-12	7	2.2	3.8			
679	Mar 9	17:16:23	GX 354-0	6	3.3	3.0	18	6.5	4.4	760	Mar 8	21:53:26	H 0614+091	3	3.8	1.6			
680	Mar 9	20:30:14	GX 354-0	5	3.0	3.6				761	Mar 9	22:53:22	4U 1812-12	14	3.3	7.7			
681	Mar 9	23:03:27	4U 1702-429	8	1.4	4.6				762	Mar 18	18:50:50	GX 354-0	6	1.9	4.1			
682	Mar 9	23:42:43	GX 354-0	5	2.0	4.2				763	Mar 19	09:50:45	GX 354-0	4	2.5	2.7			
683	Mar 10	03:04:11	GX 354-0	7	1.7	4.3				764	Mar 19	19:49:54	GX 354-0	7	2.4	3.4			
684	Mar 13	15:22:00	GX 354-0	5	2.6	3.3				765	Mar 20	22:15:00	GX 354-0	8	2.4	4.4			
685	Mar 13	20:13:24	GX 354-0	6	2.4	3.7				766	Mar 22	18:13:56	GX 354-0	5	2.5	2.3			
686	Mar 15	02:37:37	GX 354-0	5	1.8	4.1				767	Apr 6	03:14:09	GX 354-0	7	2.0	3.3	13	4.4	5.1
687	Mar 15	05:03:33	GX 354-0	5	2.8	2.9				768	Apr 6	07:01:04	GX 354-0	5	1.9	4.3			
688	Mar 15	07:35:15	GX 354-0	4	1.6	3.4				769	Apr 6	10:30:03	GX 354-0	3	2.2	2.5			
689	Mar 15	10:08:07	GX 354-0	6	3.4	3.3	7	5.2	4.5	770	Apr 6	12:11:16	IGR J17473-2721	11	1.8	6.4	26	5.6	11.8
690	Mar 15	12:19:23	GX 354-0	5	2.0	3.2				771	Apr 6	14:23:27	GX 354-0	6	3.2	3.3	10	3.9	5.6
691	Mar 15	14:18:05	GX 354-0	6	2.5	3.0	16	5.1	4.8	772	Apr 7	01:36:50	GX 354-0	5	1.9	3.1			
692	Mar 15	16:23:11	GX 354-0	4	2.5	3.1	8	3.8	4.1	773	Apr 8	13:44:47	GX 354-0	6	1.0	3.3			
693	Mar 15	19:05:31	GX 354-0	10	1.6	5.2	14	5.2	5.5	774	Apr 17	13:11:17	GX 354-0	3	2.5	2.5			
694	Mar 15	21:24:14	SAX J1712.6-3739	10	1.1	6.5				775	Aug 18	02:01:26	GX 354-0	6	2.6	3.5			
695	Mar 15	21:53:51	GX 354-0	6	2.8	3.6	15	4.6	5.7	776	Sep 10	11:58:55	GX 354-0	7	2.4	3.5			
696	Mar 16	13:14:35	GX 354-0	5	3.2	2.5				777	Sep 11	02:55:41	GX 354-0	5	2.0	3.4			
697	Mar 18	07:19:27	GX 354-0	5	2.2	2.7				778	Sep 18	10:40:24	GX 354-0	6	2.7	4.0			
698	Mar 19	01:52:02	GX 354-0	4	1.8	2.5				779	Sep 18	15:18:59	GX 354-0	5	3.0	3.0			
699	Mar 23	18:36:47	GX 354-0	4	1.1	3.2	12	2.4	4.4	780	Sep 18	20:07:34	GX 354-0	8	2.2	4.2			
700	Mar 25	01:26:18	GX 354-0	4	3.0	2.7	13	2.5	5.1	781	Sep 19	01:29:11	GX 354-0	8	1.5	4.5			
701	Apr 2	03:41:31	GX 354-0	7	1.2	3.5	11	2.9	4.9	782	Sep 20	02:33:14	GX 354-0	5	2.1	2.9			
702	Apr 2	05:58:34	SLX 1737-282	200	1.4	92.7	5	2.3	3.1	783	Sep 20	07:31:48	GX 354-0	5	1.6	3.6			
703	Apr 2	18:30:06	GX 354-0	5	1.2	3.7	8	2.8	4.1	784	Sep 20	17:03:31	GX 354-0	5	2.0	3.3			
704	Apr 4	08:32:00	GX 354-0	8	1.8	3.8				785	Sep 20	21:38:44	GX 354-0	6	1.0	3.8			
705	Apr 12	13:40:09	GX 354-0	6	2.4	3.1				786	Sep 21	02:15:18	GX 354-0	8	1.7	3.8	10	5.3	5.7
706	Aug 19	05:01:23	SAX J1810.8-2609	5	1.7	3.7				787	Sep 21	06:59:34	GX 354-0	8	2.0	4.8			
707	Aug 24	10:12:10	4U 1812-12	28	2.0	5.3				788	Sep 21	11:53:06	GX 354-0	8	1.9	4.2	41	6.1	11.8
708	Aug 27	11:36:58	GX 354-0	7	1.6	3.8				789	Sep 21	17:02:25	GX 354-0	6	3.0	3.8			
709	Aug 28	03:37:45	GX 354-0	4	2.1	2.8				790	Sep 21	22:46:09	GX 354-0	7	1.9	5.0	14	5.9	6.8
710	Aug 28	21:15:05	GX 354-0	4	1.6	2.6				791	Sep 22	07:24:26	GX 354-0	8	2.0	4.3			
711	Aug 29	12:55:57	GX 354-0	4	2.0	2.8				792	Sep 23	09:25:46	GX 354-0	6	2.0	3.3			
712	Aug 29	17:36:54	GX 354-0	5	1.0	3.5				793	Sep 23	20:31:39	GX 354-0	5	1.4	3.0			
713	Aug 29	22:43:04	GX 354-0	5	1.5	3.3				794	Sep 24	05:07:49	GX 354-0	7	3.8	4.0	13	5.5	6.1
714	Aug 30	04:22:27	GX 354-0	5	2.3	3.1	19	2.7	6.3	795	Sep 24	09:07:49	GX 354-0	6	1.5	3.9			
715	Aug 31	03:34:51	4U 1724-307	8	1.4	4.8				796	Sep 24	14:12:33	GX 354-0	8	3.1	5.4	10	4.4	6.5
716	Aug 31	04:33:54	GX 354-0	5	0.9	2.7				797	Sep 24	18:40:05	GX 354-0	6	3.5	4.0	18	4.7	6.5
717	Sep 1	11:19:28	SAX J1810.8-2609	8	3.1	4.0				798	Sep 24	22:59:13	GX 354-0	6	0.7	4.3			
718	Sep 9	14:48:22	GX 354-0	4	1.4	3.3				799	Sep 25	03:02:21	GX 354-0	6	1.4	3.9	6	4.4	3.9
719	Sep 10	15:15:44	GX 354-0	7	2.0	3.1	15	3.6	5.2	800	Sep 26	08:39:44	GX 354-0	5	2.2	3.3			
720	Sep 10	21:16:04	GX 354-0	6	1.6	3.1				801	Sep 26	21:28:23	GX 354-0	3	1.8	2.4			
721	Sep 11	12:23:19	GX 354-0	5	3.1	2.5				802	Sep 26	18:03:34	GX 354-0	4	1.7	3.3			
722	Sep 12	03:59:42	GX 354-0	6	2.3	3.6				803	Sep 26	00:40:34	GX 354-0	6	2.1	3.9			
723	Sep 12	10:52:06	GX 354-0	7	2.1	3.8													
724	Sep 13	03:48:12	GX 354-0	6	1.5	3.8													
725	Sep 13	09:11:06	GX 354-0	4	1.7	2.3													
726	Sep 13	15:22:00	GX 354-0	6	1.4	3.9	23	3.4	5.9	804	Jan 28	15:18:11	4U 1608-522	14	1.5	7.4			
727	Sep 14	03:01:10	GX 354-0	6	2.7	3.3				805	Jan 29	17:16:03	4U 1608-522	8	1.5	5.5			
728	Sep 15	02:15:49	SAX J1810.8-2609	11	1.3	7.2				806	Jan 30	04:04:23	4U 1608-522	6	2.5	4.6			
729	Sep 15	04:22:29	GX 354-0	5	1.5	3.6				807	Jan 30	13:47:34	4U 1608-522	6	2.6	2.9			
730	Sep 15	23:20:28	SAX J1810.8-2609	10	2.1	7.2				808	Jan 31	04:27:19	4U 1608-522	10	2.1	6.1			
731	Sep 16	00:44:23	GX 354-0	8	1.2	4.2				809	Jan 31	14:11:05	4U 1608-522	8	1.7	4.1	18	4.7	7.9
732	Sep 16	06:00:37	GX 354-0	4	2.4	3.0	16	3.3	5.9	810	Feb 1	03:31:41	4U 1608-522	8	1.9	4.2			
733	Sep 16	15:54:20	SAX J1810.8-2609	4	1.1	2.6				811	Feb 1	15:00:53	4U 1608-522	7	0.7	3.8			
734	Sep 16	15:56:54	GX 354-0	5	1.7	3.1	12	4.3	5.0	812	Feb 5	01:35:52	4U 1608-522	10	3.2	4.6	62	7.6	20.0
735	Sep 16	21:45:22	GX 354-0	6	1.9	3.4				813	Feb 6	10:30:41	4U 1608-522	10	2.8	5.3			
736	Sep 17	03:20:43	GX 354-0	6	3.4	3.9				814	Feb 7	02:33:56	4U 1608-522	11	2.4	6.0			
737	Sep 17	05:53:37	SAX J1810.8-2609	11	2.0	6.6				815	Feb 7	14:21:48	4U 1608-522	10	2.5	5.8			
738	Sep 20	03:31:21	4U 1812-12	15	3.6	6.2				816	Feb 7	21:56:31	4U 1636-536	7	1.4	3.2	16	3.2	6.0
739	Sep 22	09:10:57	4U 1812-12	15	2.7	7.4				817	Feb 21	21:52:31	GX 354-0	4	1.9	2.6			
740	Sep 24	01:42:08	SAX J1810.8-2609	13	1.5	6.3				818	Feb 22	18:16:42	GX 354-0	7	2.1	3.5	9	4.0	5.6
741	Sep 24	02:56:46	GX 354-0	5	1.2	3.2	14	3.6	5.2	819	Feb 22	22:10:17	GX 354-0	6	2.0	3.2	4	6	

Table 2: Burst activity of bursters in the hard X-ray energy range.

Source	N ^a	T ^b Ms	D ^c kpc	N _H ^d 10 ²² cm ⁻²	τ _h ^e d
GX 354-0	587	80.0	4.2 ^f	2.5 ¹	1.6
4U 1724-307	53	80.2	5.5 ^f	1.0 ²	17.5
4U 1702-429	48	74.0	4.5	5.0 ³	17.8
4U 1608-522	37	71.2	3.8	1.2 ⁴	22.3
4U 1636-536	23	70.8	5.1	0.3 ⁵	35.6
4U 1812-12	23	65.6	3.6 ^f	1.6 ⁶	33.0
SAX J1810.8-2609	15	80.5	5.4	0.3 ⁷	62.1
1A 1743-288	8	81.5	5.6	8.8 ⁸	118.0
Aql X-1	6	72.1	5.1 ^f	0.3 ⁵	139.0
SLX 1735-269	4	79.9	5.3 ^f	1.3 ⁹	231.0
KS 1741-293	4	81.4	6.2	20.0 ¹⁰	236.0
SAX J1712.6-3739	4	78.9			228.0
XB 1832-330	4	82.8	9.5	0.2 ¹¹	240.0
SLX 1737-282	3	80.7	5.4	1.9 ¹²	311.0
2S 0918-549	3	90.6			350.0
SLX 1744-299/300	2	81.7			573.0
H 0614+091	2	127.0			735.0
3A 1850-087	2	69.1			400.0
GX 17+2	1	68.4			792.0
GX 3+1	1	80.4	6.4	1.6 ¹³	931.0
IGR J17380-3749	1	79.6			921.0
AX J1754.2-2754	1	81.8	5.6 ^f	2.1 ¹⁴	947.0
3A 1246-588	1	81.2			940.0
IGR J17473-2721	1	79.8	4.4	3.8 ¹⁵	924.0

^a The number of bursts recorded from the source.^b The total exposure time of the source observation.^c The upper limit on the distance to the source.^d The interstellar absorption adopted for the source.^e The recurrence period of "hard" bursts from the source.^f Distance to the source was estimated based on the photospheric expansion burst.

[1] - Di Salvo et al., 2000, [2] - Barret et al., 1999, [3] - Makishima et al., 1982,

[4] - Tarana et al., 2008, [5] - Dickey and Lockman, 1990, [6] - Barret et al., 2003,

[7] - Jonker et al., 2004, [8] - Werner et al., 2004, [9] - David et al., 1997,

[10] - Sidoli et al., 1999, [11] - Parmar et al., 2001, [12] - in't Zand et al., 2002,

[13] - Oosterbroek et al., 2001, [14] - Sakano et al., 2002, [15] - Altamirano et al., 2008.